Bridging the gap between atmospheric concentrations and local ecosystem measurements

Lauvaux, T.; Gioli, B.; Sarrat, C.; Rayner, P.J.; Cias, P.; Chevallier, F.; Noilhan, J.; Miglietta, F.; Brunet, Y.; Ceschia, E.; Dolman, A.J.; Elbers, J.A.; Gerbig, C.; Hutjes, R.W.A.; Jarosz, N.; Legain, D.; Uliasz, M.

published in
Geophysical Research Letters
2009

DOI (link to publisher)
10.1029/2009GL039574

document version
Publisher's PDF, also known as Version of record

GEOPHYSICAL RESEARCH LETTERS, VOL. 36, L19809, doi:10.1029/2009GL039574, 2009

Bridging the gap between atmospheric concentrations and local ecosystem measurements

T. Lauvaux,[1,2,3] B. Gioli,[4] C. Sarrat,[2] P. J. Rayner,[1] P. Ciais,[1] F. Chevallier,[1] J. Noilhan,[2] F. Miglietta,[4] Y. Brunet,[5] E. Ceschia,[6] H. Dolman,[7] J. A. Elbers,[8] C. Gerbig,[9] R. Hutjes,[8] N. Jarosz,[10] D. Legain,[2] and M. Uliasz[11]

Received 11 June 2009; revised 12 August 2009; accepted 27 August 2009; published 15 October 2009.

[1] This paper demonstrates that atmospheric inversions of CO_2 are a reliable tool for estimating regional fluxes. We compare results of an inversion over 18 days and a 300 × 300 km^2 domain in southwest France against independent measurements of fluxes from aircraft and towers. The inversion used concentration measurements from 2 towers while the independent data included 27 aircraft transects and 5 flux towers. The inversion reduces the mismatch between prior and independent fluxes, improving both spatial and temporal structures. The present mesoscale atmospheric inversion improves by 30% the CO_2 fluxes over distances of few hundreds of km around the atmospheric measurement locations. **Citation:** Lauvaux, T., et al. (2009), Bridging the gap between atmospheric concentrations and local ecosystem measurements, *Geophys. Res. Lett.*, *36*, L19809, doi:10.1029/2009GL039574.

1. Introduction

[2] Atmospheric inversions have played a key role in quantifying large-scale sources and sinks of CO_2 [e.g., *Tans et al.*, 1990; *Gurney*, 2002; *Baker et al.*, 2006]. There are no direct measurements of CO_2 flux at these large scales so the information cannot be verified. This paper attempts such an evaluation at the mesoscale, over a limited area. We immediately face a problem of scale since we need sufficiently dense flux measurements to obtain spatial estimates comparable with the atmospheric inversions. During the CarboEurope Regional Experiment Strategy (CERES) in Southern France [*Dolman et al.*, 2006], CO_2 surface fluxes and atmospheric concentrations were measured at several locations. Two towers measured continuously CO_2 concentrations near the coast and inland (see auxiliary material: Text S1, section 4) (Figure 1).[12] For fluxes, five ground sites were selected to represent the main regional ecosystem types, and two transects were repeatedly measured by aircraft flying at low altitude. The surface footprints of the aircraft fluxes are of comparable scales to the inversion resolution, and are considered as the reference flux measurements in this study. The direct flux measurements (from both aircraft and towers) are completely independent of the inversion and are kept as validation data for the inverse fluxes. Daytime averages are calculated at 8 km resolution over three 6-day periods using hourly CO_2 measurements and high-resolution transport modelling (see Text S1, section 1). The temporal resolution is a compromise due to the lack of data (only two atmospheric concentration towers) but still uses the information from hourly concentrations. *Sarrat et al.* [2007b] and *Lauvaux et al.* [2009] demonstrated the capability of the model to assimilate such observations.

[3] This study uses three different types of flux estimates: the two different types of flux measurements, from the towers close to the surface (Method 1a), and from the aircraft flying at 200m high (Method 1b), and the inverse fluxes that are based on atmospheric measurements referred as Method 2. Technical details on the inverse system or on the measurement characteristics are given in the auxiliary material.

[4] The outline of the paper is as follows: In Section 2, we briefly describe the tools and data sets underlying the study. Section 3 describes the major results while Section 4 considers some implications and summarises the results.

2. Inverse System and Independent Flux Measurements

[5] The study period consists of 18 days in 2005 divided into 3 Intensive Observing Periods, IOP-1 (May 24–29), IOP-2 (May 30–June 4) and IOP-3 (June 5–10). We estimate mean daytime fluxes for each IOP at 8 × 8 km resolution (between 8 am and 8 pm). For the Method 2, we used hourly concentrations that were measured on two towers throughout the period (Figure 1). Influence functions of these two towers, describing the relation between surface fluxes and concentrations, are calculated using the non hydrostatic atmospheric model Meso-NH [*Lafore et al.*, 1998] coupled to the Lagrangian model LPDM [*Uliasz*, 1994] (see Text S1, section 1). The typical surface flux area influencing the tower's concentration measurements

[1]Laboratoire des Sciences du Climat et de l'Environnement, Gif-sur-Yvette, France.
[2]CNRM, Météo France, Toulouse, France.
[3]Now at Department of Meteorology, Pennsylvania State University, State College, Pennsylvania, USA.
[4]Institute of Biometeorology, CNR, Florence, Italy.
[5]INRA, EPHYSE, Bordeaux, France.
[6]CESBIO, Toulouse, France.
[7]Department of Hydrology and Geo-environmental Sciences, Vrije Universiteit, Amsterdam, Netherlands.
[8]Centre for Water and Climate, Alterra, Wageningen University and Research Centre, Wageningen, Netherlands.
[9]Max Planck Institute for Biogeochemistry, Jena, Germany.
[10]CESBIO, Auch, France.
[11]Department of Atmospheric Science, Colorado State University, Fort Collins, Colorado, USA.

0094-8276/09/2009GL039574$05.00

[12]Auxiliary materials are available in the HTML. doi:10.1029/2009GL039574.

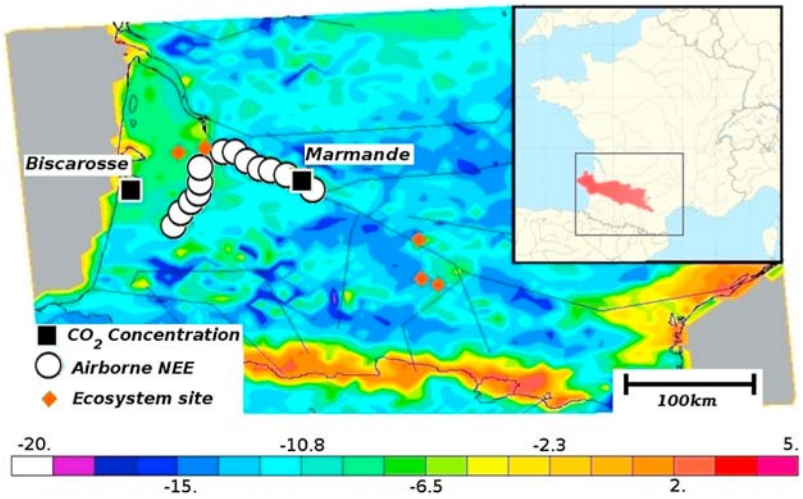

Figure 1. Averaged daytime NEE (in μmol.m^{-2}.s^{-1}) from ISBA vegetation scheme (first guess) for IOP-1 with the two concentration towers (black squares), the CO_2 flux towers (red diamonds), and the aircraft surface footprint (white circles). The influence function of the two concentration towers for IOP-1 is indicated in red on the map (inset).

extends 300 km from the Atlantic Ocean to the Mediterranean coast (Figure 1, inset, in red). The first guess fluxes are computed each hour with the ISBA-A-gs land surface model [*Calvet et al.*, 1998] at 8 km resolution, forced by the SAFRAN meteorological analyses [*Durand et al.*, 1993]. Concentration boundary conditions from the inversion come from a run of the LMDZ global model [*Sadourny and Laval*, 1984]. Boundary conditions are included in the inversion but have little impact in our domain [*Lauvaux et al.*, 2009].

[6] The Method 1b consists of 27 airborne transects that were made during the study period to measure CO_2 surface fluxes over the same paths [*Gioli et al.*, 2004] (see Text S1, section 6.2). Figure 1 illustrates the two airborne flux transects over the pine-forest ecosystem of Les Landes and the agricultural area of Marmande. And finally, for the Method 1a, we select five instrumented flux towers corresponding to the ecosystem types of the aircraft paths, Auradé and Lamasquère (cereals), Marmande and Saint Sardos (maize), at 2.5 to 6 m height, and Le Bray (pine forest) at 40 m height to characterize the representative ecosystems of the flights over the region (see Text S1, section 5).

[7] Spatial averaging from Method 1b produces aggregated fluxes at about 4 km scale and it is these that we compare with our inversions. Even though the inversion scale is larger (8 km), they both remain much larger than the average agricultural plot scale (about 0.3 km) which avoids representation error. Considering Method 1a, the corresponding spatial scale is much smaller (usually equivalent to the agricultural plot). We compare the fluxes when related to similar ecosystem types, even if the location differs. We assume that spatial variability is much smaller than temporal behaviour for a given ecosystem. For the larger scales (Methods 1b and 2), the ecosystem type is the dominant type that covers at least 30% of the pixel.

3. Results

[8] We compare the prior and posterior daytime NEE of Method 2 to the airborne observations (Method 1b) and to the flux tower measurements (Method 1a). The temporal resolution is limited to 6 days due to the scarcity of concentration observations. Figure 2 shows the 6-day mean corrected fluxes during the day for the forest ecosystems (deciduous and coniferous types), and agricultural ecosystems composed by winter crops (C_3, mainly cereals) and summer crops (C_4, mainly maize), with their associated standard deviations. The three IOP show significant trends in the averaged daytime NEE from Method 1b and Method 1a, corresponding to the rapid growth of summer crops starting in the IOP-3 (5 to 10 June). The trend in airborne NEE of increasing CO_2 uptake resembles the C_4 crop ecosystem flux measurements (from -3 μmol.m^{-2}.s^{-1} for IOP-1 to -8 μmol.m^{-2}.s^{-1} for IOP-2). The C_3 crop flux site NEE shows a decrease of the CO_2 uptake (from -11 to -8 μmol.m^{-2}.s-1).

[9] Posterior NEE from Method 2 is closer to the airborne observations than is the prior of the vegetation model for all the IOP shown in Figure 2. Even though prior NEE is better for the forest than for the crops (only 2 to 4 μmol.m^{-2}.s-1 error, i.e., 50% of the absolute NEE), the posterior NEE of Method 2 still lies closer to the ecosystem observations. Posterior errors are 20% to 50% less than prior errors. The improvement occurs despite only having two concentration measurement series.

[10] At 8 km grid resolution, 14 inversion grid points lie on the two repeated aircraft transects (Figure 1). Figure 3 shows the corrected fraction ρ of the initial misfit ($\rho = (\varepsilon_{corrected} - \varepsilon_{first\ guess})/\varepsilon_{first\ guess}$ with $\varepsilon = |NEE_{model} - NEE_{observed}|$ the model-data mismatch) at these locations between Method 2 and Method 1b. Negative values indicate an improvement, which is observed at 9 out of 14 different locations in our case. Over the three IOP (i.e., 3 time periods multiplied by 14 locations), 31 out of 42 differences show an improvement by the Method 2 compared to Method 1b. This metric penalizes cases with good priors such as the Les Landes forest (Western transect). The agricultural area (Eastern transect) shows better agreement for all locations (from 10 to 60% of reduction of the initial misfit in Figure 3). Both first guess and corrected flux estimates lie

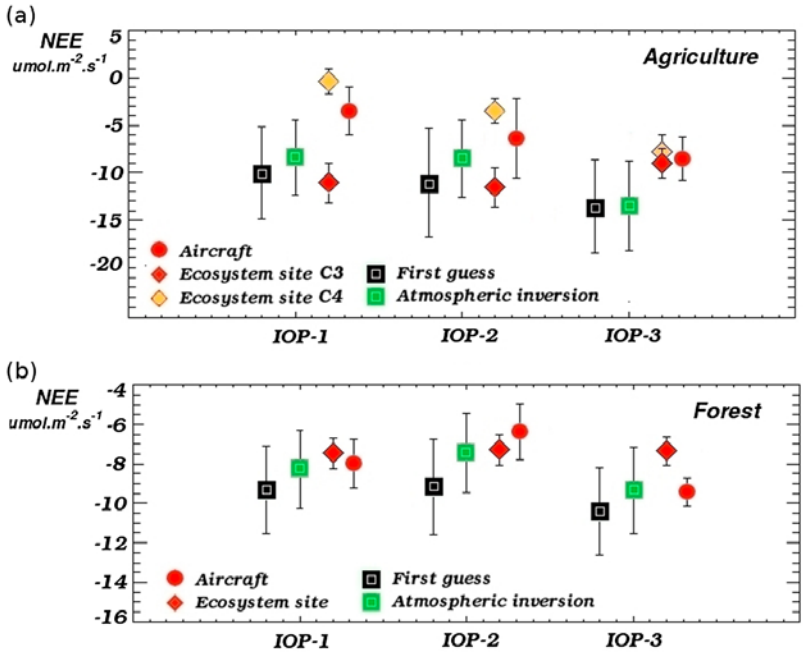

Figure 2. Averaged daytime NEE (in μmol.m^{-2}.s^{-1}) from the land surface model (first guess) and the corrected fluxes (Method 2) compared to the daytime NEE observed from the aircraft (Method 1b) and the 5 flux towers (Method 1a) for (top) agricultural area fluxes with summer and winter crops (aggregated in the aircraft flux) and (bottom) forest ecosystem fluxes including deciduous and coniferous forest types in the model (first guess and corrected fluxes). Error bars for the direct measurements (Methods 1a and 1b) correspond to the 95% confidence interval.

close to the flux measurements, but relative to the posterior uncertainty.

[11] We finally combine the spatial and temporal comparisons into an overall statistical measure of inversion performance (Method 2). Figure 4 shows this statistical comparison for all the evaluation ecosystem NEE measurements (Methods 1a and 1b) and the inversion during daytime (Method 2). Along the x-axis (from left to right), we show the prior misfit averaged from the vegetation model over all the aircraft locations and the same estimate

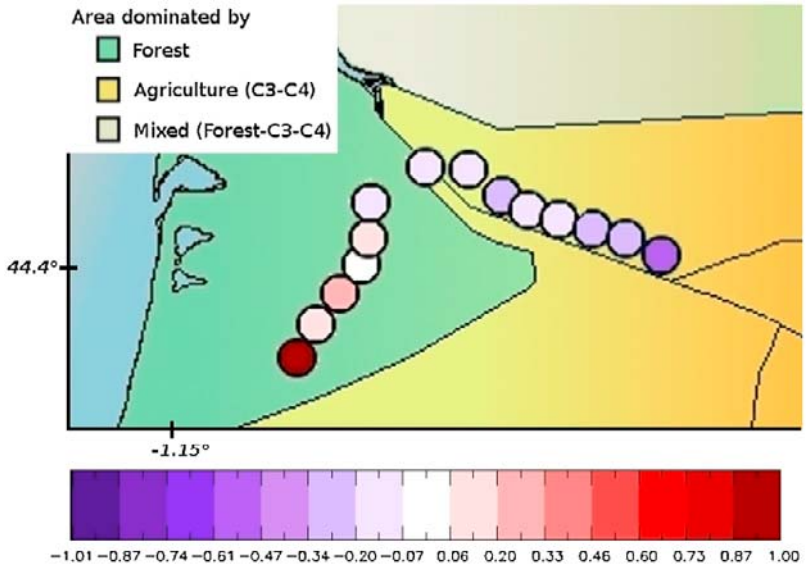

Figure 3. Normalized fractions ρ of the inverse daytime NEE at the aircraft locations, negative if improved (reduction of the initial misfit) and positive when degraded, i.e., ratios of the difference between the corrected fluxes and the aircraft ($\varepsilon_{corrected}$) minus the first guess and the aircraft ($\varepsilon_{first\ guess}$) normalized by the prior misfit (($\varepsilon_{corrected} - \varepsilon_{first\ guess}$)/$\varepsilon_{first\ guess}$). The area dominated by forest ecosystem types is indicated in green, by agriculture is indicated in orange, and by mixed forest with crops is indicated in grey.

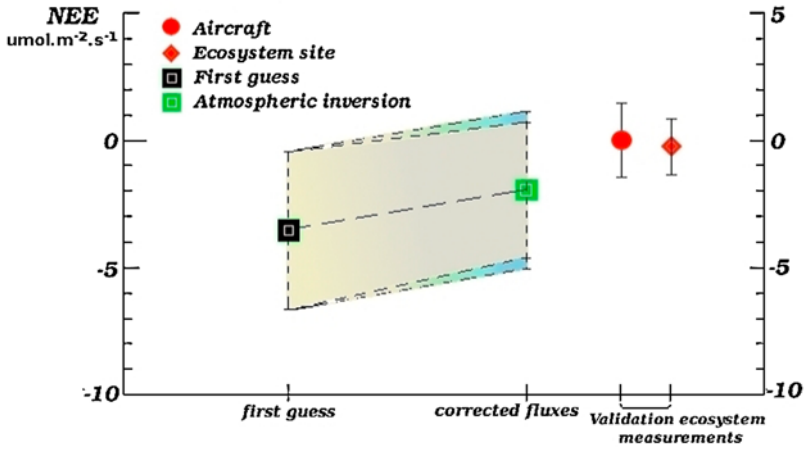

Figure 4. Comparison of the model misfit for the prior (first guess from the vegetation model ISBA-A-gs) and the posterior (corrected fluxes from the inversion) of daytime NEE (in μmol.m^{-2}.s^{-1}) to the aircraft and tower flux data (aircraft NEE being the reference, equal to 0). At each aircraft flux location, the normalized distance was summed, indicated on the figure as error bars, $\Sigma = \frac{(NEE_{model} - NEE_{aircraft})2}{\sigma_{NEEmodel}}$, following the χ^2 distribution law. The fit between theoretical error reduction and observed improvement of the flux estimate is shown by the decrease of the normalized distance of the posterior NEE (in blue). Estimates have no x-axis correspondence.

after the inversion. The error bars represent the mean square observed error of the prior and the posterior, divided by their respective theoretical standard deviations (prior and posterior uncertainties). This ratio tests the consistency of the inversion since it requires that, where the posterior error is smallest (i.e., the atmosphere provides most information) the match to independent flux measurements is most improved. The improvement in corrected fluxes is hence larger than the decrease of flux uncertainty suggesting that transport model error was slightly overestimated by the concentration data comparison. Finally, the two types of flux observations (Methods 1a and 1b) are on the right side of the x-axis. The inversion decreases first guess misfit from 4 to 2 μmol.m^{-2}.s^{-1} (25% of the mean NEE) and reduces the NEE error by 15% over the area visible to the atmosphere (Figure 1).

4. Discussion and Conclusions

[12] The results suggest that when compared to direct flux measurements at comparable scales (Method 1b), the atmospheric inversion significantly improves the prior estimates; even where the prior is fairly good. Improvement occurs for both spatial structure and time evolution. This is true despite only having two concentration time series and despite the heterogeneity of the landscape. The agreement with Method 1a is similar to Method 1b, and shows that the regional study allows the use of flux measurements with smaller spatial representativity, if using ecosystem types that dominate the area.

[13] One reason for the apparent success may be that the major components of the inversion system had been previously tested and the relevant uncertainties assigned accordingly. Prior uncertainties were assigned by comparison with observations. The uncertainties on data were set by considering the mismatch between simulations and observations calculated by *Sarrat et al.* [2007a] and *Lauvaux et al.* [2009] using the prior fluxes. This is a conservative choice since some of this mismatch comes from errors in the prior flux. We also account for some of the uncertainty in transport [*Lauvaux et al.*, 2008]. Finally, *Lauvaux et al.* [2009] has also shown that much of the domain is observable from the two measurement sites. Our results suggest that, if these conditions (reasonable prior, good transport and reasonable signal) are met, the inversion is likely to produce meaningful results.

[14] Finally, this study supports the use of aircraft flux measurements. Such measurements seem to be less constrained by representation problems than pointwise flux tower measurements. Although they cannot be used as a routine tool for monitoring regional fluxes, a combination of flux towers validating aircraft fluxes, which in turn validate atmospheric inversions, seems to provide the link between small and large scales required for quantifying and understanding regional carbon balances.

[15] **Acknowledgments.** We wish to thank all participants in the CERES campaign for making their data freely available (http://carboregional.mediasfrance.org/campagne/index). This work was funded by the European Commission, Sixth Framework Programme, contract GOCE-CT-2003-505572.

References

Baker, D. F., et al. (2006), TransCom 3 inversion intercomparison: Impact of transport model errors on the interannual variability of regional CO_2 fluxes, 1988–2003, *Global Biogeochem. Cycles*, *20*, GB1002, doi:10.1029/2004GB002439.

Calvet, J. C., J. Noilhan, J. L. Roujean, P. Bessemoulin, M. Cabelguenne, A. Olioso, and J. P. Wigneron (1998), An interactive vegetation SVAT model tested against data from six contrasting sites, *Agric. For. Meteorol.*, *92*, 73–95.

Dolman, A. J., et al. (2006), CERES, the CarboEurope Regional Experiment strategy in les Landes, south west France, May–June 2005, *Bull. Am. Meteorol. Soc.*, *87*, 1367–1379, doi:10.1175/BAMS-87-10-1367.

Durand, Y., E. Brun, L. Mérindol, G. Guyomarc'h, B. Lesaffre, and E. Martin (1993), A meteorological estimation of relevant parameters for snow models, *Ann. Glaciol.*, *18*, 65–71.

Gioli, B., et al. (2004), Comparison between tower and aircraft-based eddy covariance fluxes in five European regions, *Agric. For. Meteorol.*, *127*, 1–16.

Gurney, K. R. (2002), Towards robust regional estimates of CO_2 sources and sinks using atmospheric transport models, *Nature*, *415*, 626–630.

Lafore, J., et al. (1998), The Meso-NH atmospheric simulation system. Part I: Adiabatic formulation and control simulations, *Ann. Geophys.*, *16*, 90–109.

Lauvaux, T., M. Uliasz, C. Sarrat, F. Chevallier, P. Bousquet, C. Lac, K. J. Davis, P. Ciais, A. S. Denning, and P. Rayner (2008), Mesoscale inversion: First results from the CERES campaign with synthetic data, *Atmos. Chem. Phys.*, *8*, 3459–3471.

Lauvaux, T., O. Pannekoucke, C. Sarrat, F. Chevallier, P. Ciais, J. Noilhan, and P. J. Rayner (2009), Structure of the transport uncertainty in mesoscale inversions of CO_2 sources and sinks using ensemble model simulations, *Biogeosciences*, *6*, 1089–1102.

Sadourny, R., and K. Laval (1984), January and July performance of the LMD general circulation model, in *New perspectives in Climate Modeling*, edited by A. L. Berger and C. Nicolis, pp. 173–197, Elsevier, Amsterdam.

Sarrat, C., et al. (2007a), Atmospheric CO_2 modeling at the regional scale: An intercomparison of 5 meso-scale atmospheric models, *Biogeosciences*, *4*, 1115–1126.

Sarrat, C., J. Noilhan, P. Lacarrère, S. Donier, H. Dolman, C. Gerbig, P. Ciais, and A. Butet (2007b), Atmospheric CO_2 modeling at the regional scale: Application to the Carboeurope Regional Experiment, *J. Geophys. Res.*, *112*, D12105, doi:10.1029/2006JD008107.

Tans, P. P., I. Y. Fung, and T. Takahashi (1990), Observational constraints on the global atmospheric CO_2 budget, *Science*, *247*, 1431–1438.

Uliasz, M. (1994), Lagrangian particle modeling in mesoscale applications, in *Environmental Modelling: Computer Methods and Software for Simulating Environmental Pollution and Its Adverse Effects*, vol. 2, edited by P. Zanetti, pp. 71–102, Comput. Mech. Publ., Boston, Mass.

Y. Brunet, INRA, EPHYSE, BP 81, 71 rue Edouard Bourleaux, F-33883 Villenave d'Ornon CEDEX, France.

E. Ceschia, CESBIO, UMR 5126, Unité Mixte CNES/UPS/IRD/CNRS, Room 112, 18 avenue Edouard Belin, F-31401 Toulouse CEDEX 9, France.

F. Chevallier, P. Ciais, and P. J. Rayner, Laboratoire des Sciences du Climat et de l'Environnement, IPSL, UVSQ, UMR 1572, F-91191 Gif-sur-Yvette, France.

H. Dolman, Department of Hydrology and Geo-environmental Sciences, Vrije Universiteit, NL-1081 HV Amsterdam, Netherlands.

J. A. Elbers and R. Hutjes, Centre for Water and Climate, Alterra, Wageningen University and Research Centre, NL-6700 AA Wageningen, Netherlands.

C. Gerbig, Max Planck Institute for Biogeochemistry, Hans-Knoell Strasse 10, D-07745 Jena, Germany.

B. Gioli and F. Miglietta, Institute of Biometeorology, CNR, Via Giovanni Caproni, 8, I-50145 Florence, Italy.

N. Jarosz, CESBIO, UMR 5126, Unité Mixte CNES/UPS/IRD/CNRS, Room 112, 24 rue d'Embaquès, F-32000 Auch, France.

T. Lauvaux, Department of Meteorology, Pennsylvania State University, State College, PA 16802, USA. (lauvaux@meteo.psu.edu)

D. Legain, J. Noilhan, and C. Sarrat, CNRM, Météo France, 42 avenue G. Coriolis, F-31057 Toulouse CEDEX, France.

M. Uliasz, Department of Atmospheric Science, Colorado State University, Fort Collins, CO 80523, USA.